EGTRIB Journal
JOURNAL OF
THE EGYPTIAN SOCIETY OF TRIBOLOGY
VOLUME 9, NO. 3, JULY 2012, pp. 40 - 52 **ISSN 2090 - 5882**

SAND EROSION TESTING OF POLYMERIC COATINGS OF STEEL SHEETS

Al-Qaham Y., Breemah A., Mohamed M. K. and Ali W. Y.

Faculty of Engineering, Taif University, Saudi Arabia.

ABSTRACT

The sand erosion testing of transparent polymeric coatings of steel sheets was investigated. The tested coatings were aimed to coat the vehicle surfaces as well as lamp covers to defeat sand erosion during dusty storms. An air-sand erosion test rig was designed and manufactured for that purpose. The test rig was designed to allow constant velocity of sand particles to impact the coated steel sheets. Four types of transparent polymeric coatings (A, B, C and D) were tested. The evidence of erosion caused by sand particles in the coating surfaces was inspected before and after test by optical microscope.

Based on the experimental results, it is found that the tested coatings (A) and (B) showed significant wear decrease. The lowest wear values were observed for coating thickness of 0.08 mm. At 90 ° angle of inclination embedment of sand particle was indicated by the weight increase after test. Heat treatment of the coatings caused significant wear decrease. Wear decreased down to minimum then remarkably increased with increasing angle of inclination. Coating (C), at low angle of inclination, showed relatively high wear resistance. This means that the shear strength of the coating is relatively high. As the angle of inclination increased wear increased. Heat treatment of coating (C) slightly decreased wear, where minimum values were observed at 60° angle of inclination.

KEYWORDS

Erosion, sand particles, steel sheets, transparent polymeric coatings, thickness, angle of inclination, heat treatment.

INTRODUCTION

Frequently aircraft, tank and helicopter gas turbine engines are operated in a desert environment where the gas turbine compressor rotor blades and vanes are exposed to erosive media such as sand and dust. Base metal erosion leads to increased fuel consumption, efficiency loss, and can cause damage to compressor and turbine hardware. Erosion resistant coatings can be used to prolong the life of compressor airfoils in a sand erosion environment, [1]. The key features of two selected coating architectures are outlined. Selected erosion performance data with different erosion media are presented. Excellent mechanical properties of single layer nitride coating such as high hardness and Young's modulus make it a very attractive material for the protection against the different types of wear, [2]. Mechanisms of solid particle erosion of metals and brittle materials, such as Ti-N and other nitride coatings have been

discussed. It was demonstrated that the erosion rate of brittle coating compared to ductile coatings is lower at low impact angle but is higher at high impact angle, [3]. Brittle/ductile multilayer systems have also been applied successfully in commercial applications.

The sand erosion rates of novel compositions of hard ceramics such as tungsten carbide, silicon nitride, silicon carbide, and partially stabilized zirconia have been tested in air-sand erosion facilities. A new testing facility that ensured stable and reproducible erosion testing with sand velocities and concentrations up to 250 m/s and 5 wt. % in air, respectively, was built, [4]. Special rig design features allowed accurate sand consumption monitoring during each test. High-speed photography was used to determine the sand velocity distribution at each test setting. High-speed visualization of the sand impact on the material surface demonstrated fragmentation of almost every sand particle in the range of velocities of 60 m/s and higher. The evidence of extensive fragmentation contributed to understanding the origin of the erosion resistance of hard ceramics.

Selection of materials capable of withstanding sand erosion is one of the major problems encountered when designing valves for oil and gas severe service applications, [5 - 7]. The erosion problem is particularly acute for gas choke valves where natural gas, initially compressed to 200 - 500 kp/cm^2, may reach sonic velocity within the choke trim. The enormous fluid velocity accelerates entrained sand particles that subsequently impinge onto walls of the valve parts as well as the downstream pipe work.

The angle dependence of the erosion rate was obtained by testing the materials at an impact angle of 30◦ with the sand velocity of 105 m/s. It is generally believed, [8, 9] that for brittle materials such as hard ceramics a maximum erosion rate occurs at 90°, whereas for ductile materials this occurs at oblique impact angles. The erosion rate increases with the sand concentration because of the increased opportunity of sand particles impacting the steel surface, [10]. It was proposed, [11], that during each impact, plastic deformation takes place at the vicinity of the impact when the yield strength of steel is locally exceeded. Multiple impacts could generate a plastically deformed layer near the eroded surface with the increased yield strength due to strain hardening, reducing the erosion rate.

A single correlation for sand erosion of a "family" of polyurethanes is presented. By "family" is meant a group of chemically similar compounds, [12]. The natural time of a viscoelastic fluid: its significance and measurement, observations regarding the number of dimensional parameters in viscoelastic constitutive equations has been used together with the Pi theorem to prepare a single dimensionless correlation for a group of materials with similar but different forms of constitutive equations, different forms of stress-deformation behavior. Results of a large number of erosion tests on artificially generated and relatively dense sand–mud mixtures are presented, [13]. Soil sample compositions are varied concerning clay–silt and sand–silt ratio, and clay mineralogy. An experimental approach to accelerated laboratory testing sand erosion in high pressure flow channels of complicated 3D configurations was developed, [14]. The channels were designed for erosion-resistant valves in natural gas and oil severe service applications. A testing facility that operated at 40 bar of nitrogen pressure with silica sand as an erodent was built and calibrated. The flow channels were manufactured from organic glass (PMMA) in separate plates that facilitated weight loss measurements in

different parts of the channels as well as erosion visualization. The particular grade of glass was selected after testing erosion in a range of materials in order to find close resemblance to stainless steel in terms of both the erosion rate angle function and the velocity exponent.

The operating environment in Middle East is particularly severe in terms of the high ambient dust concentrations experienced throughout the Eastern and Western Provinces, [15]. During severe dust storm conditions dust concentrations of the order of 100 to 500 times higher may be encountered. It was found that the vast majority of airborne in the Eastern Province are concentrated in the smaller sizes. 95 % of all particles are below 20 μm and 50 % of all particles are below 1.5 μm in size. The dusty storms continue for long times in Gulf area. The erosion of vehicles body has an accelerated rate.

In the present research, it is aimed to investigate four types of polymeric transparent coating materials to resist the erosive wear caused by sand particles. The angle of inclination of the test specimens, the thickness of the coating and the effect of heat treatment are investigated.

EXPERMENTAL

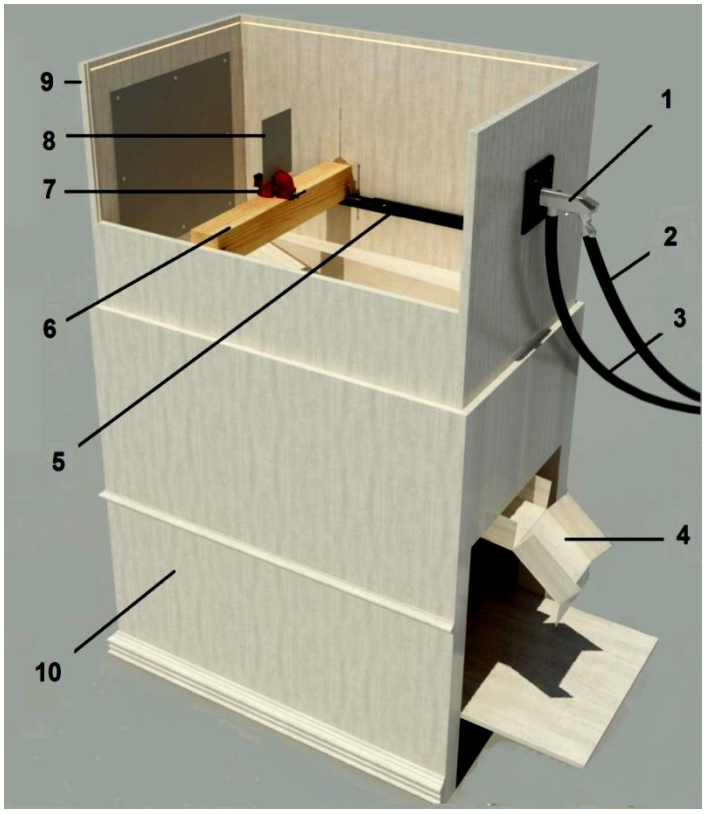

1. Sand blaster gun.
2. Hose connected to the compressor.
3. Hose connected to the reservoir.
4. To drain.
5. Linear bearings.
6. Beam.
7. Parallel jaw vise.
8. Specimen.
9. Test chamber.
10. Stand.

Fig. 1 Details of the test rig.

An air compressor was used to compress atmospheric air to 0.8 N/mm^2 (8 bar) maximum pressure. The air was stored in a pressure vessel of 25 litres capacity. The compressor refilled automatically when the pressure decreases to 7 bar. A sand blaster gun (1) was used to eject air mixed with sand. There were two hoses. The first hose (2) was connected to the bottom of the handle and to the compressor, while the second hose

(3) was connected to the bottom of the barrel and attaches the underside of a reservoir that contains sand particles. When the trigger of the gun was pressed, the air passed from the pressure vessel created a suction ejecting the sand particles up to the hose from its reservoir through a 3 mm diameter nozzle. The average velocity of the air mixed with the sand particles were calculated (30 m/s, 108km/h). The details of the test rig are shown in Fig. 1.

The sand blaster gun was fixed to one side of a test chamber (9) which was a 450 mm height, 500 mm width and 780 mm long. The specimens were held by a parallel jaw vice (7) fixed inside the test chamber on adjustable beam that can be moved forward and backward from the nozzle depending on the distance needed. In this study the distance from the tip of the nozzle to the centre line of the parallel jaw vice was fixed to 600 mm. The test chamber was placed on a stand with a fixed drain (5) to collect sand. The duration of the sand blast was 2.0 seconds. The sand was sieved before the test to control the particles size up to 2.0 mm. Sand was collected from the western desert in Saudi Arabia.

The tested specimens were made of low carbon steel (St. 37.11, DIN 1611), where their dimensions were 100 × 100 mm and 0.6 mm thickness. The test specimens were bended to 5 different inclination angles of 10°, 20°, 40°, 60°, 90°. Four types of coating materials were tested (A, B, C and D). They were polymeric transparent types.

RESULTSAND DISCUSSION

The wear of the tested coating (A) is shown in Fig. 2. The thicknesses of the coating were 0.03, 0.05 and 0.11 mm, where the highest thickness displayed minimum wear at 60° angle of inclination. This behavior might be attributed to the increase of embedment of sand particles in coating surface as its thickness increased. Heat treatment of coating (A) up to 50 °C enhanced wear resistance of the coating, Fig. 3.

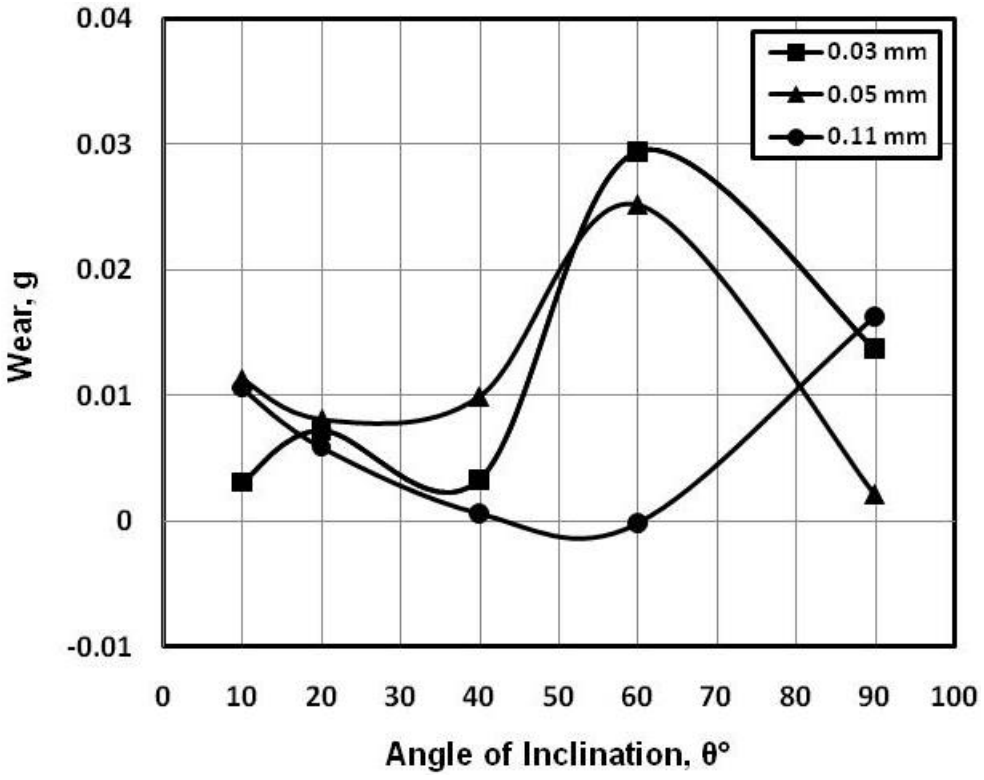

Fig. 2 Wear of coating (A) versus angle of inclination.

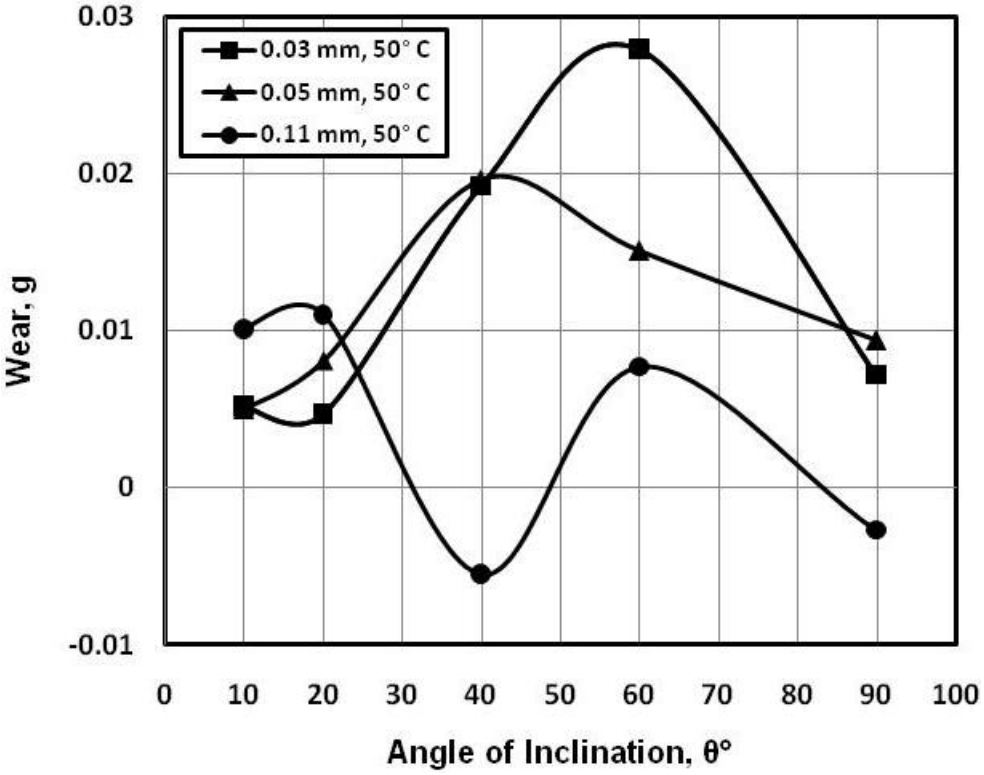

Fig. 3 Wear of coating (A) after heat treatment (50 °C) versus angle of inclination.

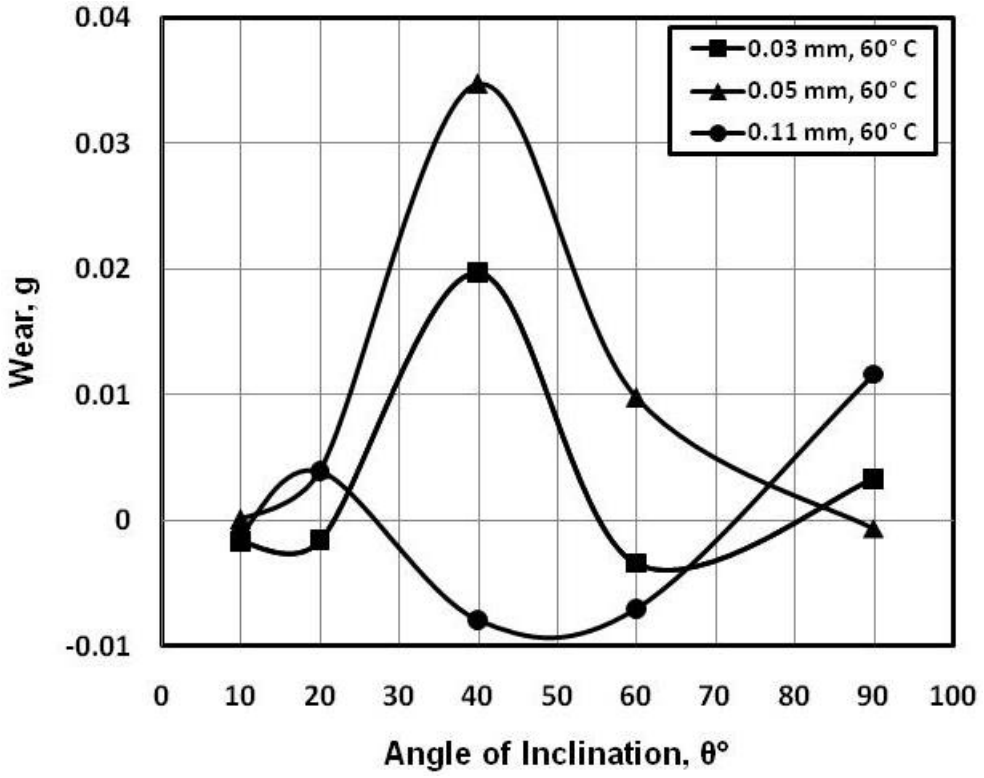

Fig. 4 Wear of coating (A) after heat treatment (60 °C) versus angle of inclination.

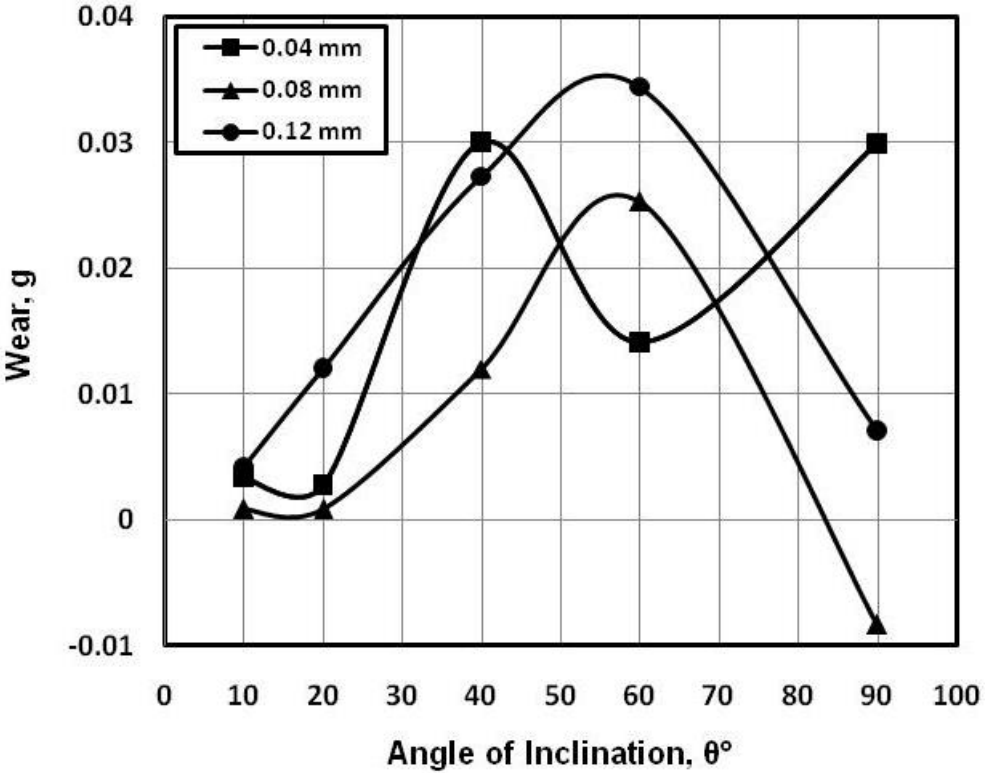

Fig. 5 Wear of coating (B) versus angle of inclination.

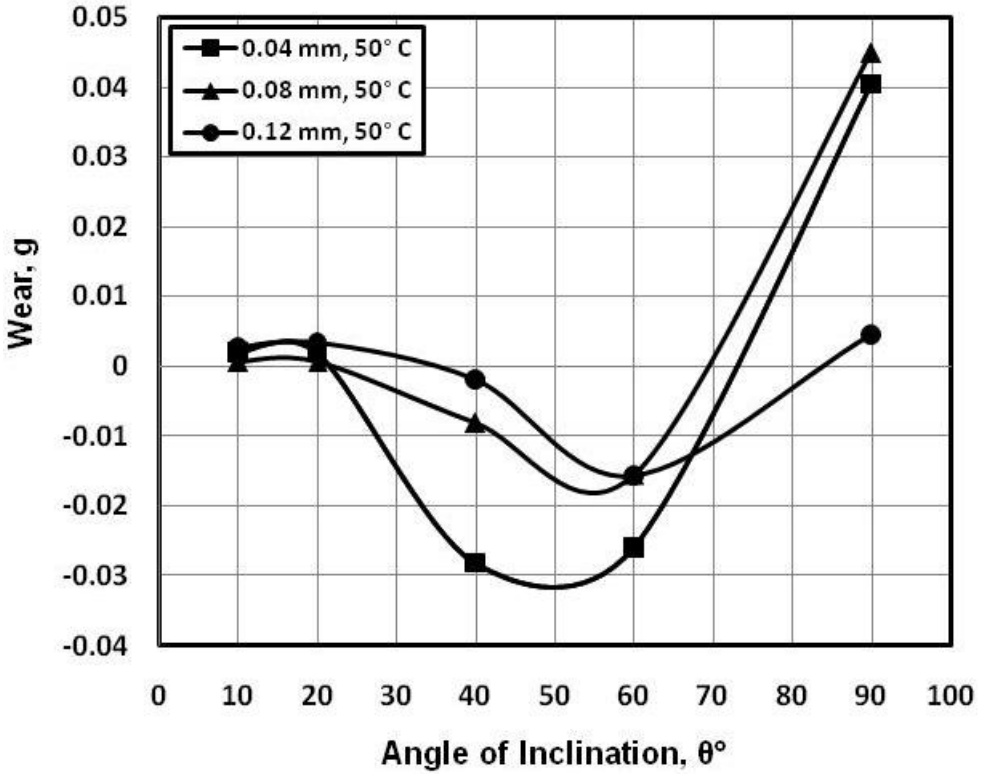

Fig. 6 Wear of coating (B) after heat treatment (50 °C) versus angle of inclination.

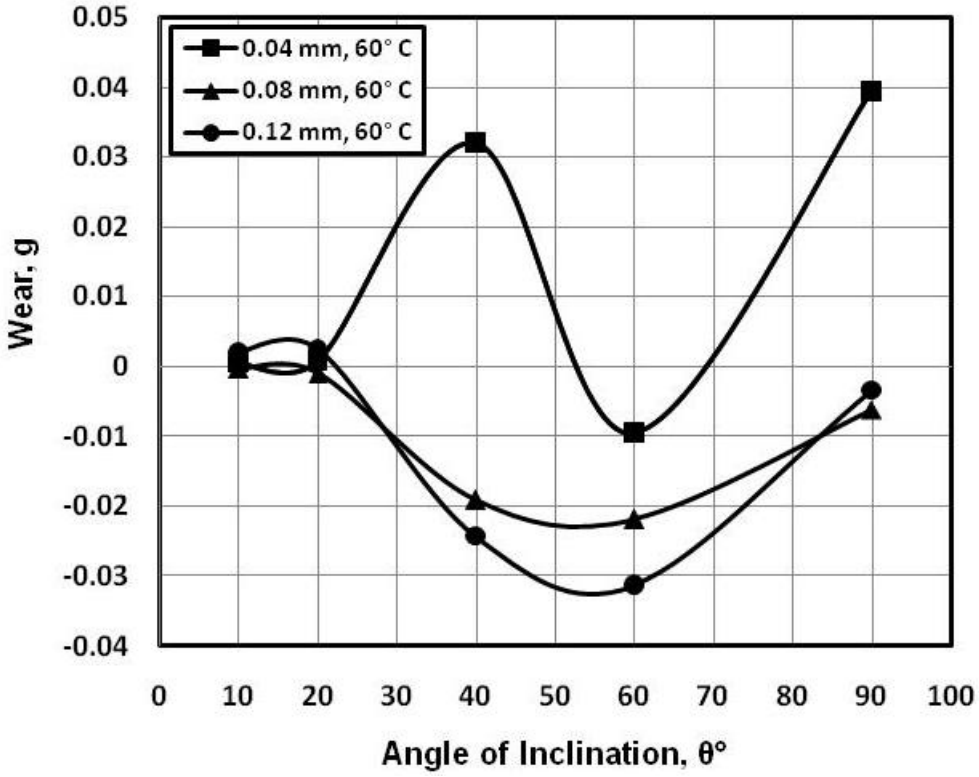

Fig. 7 Wear of coating (B) after heat treatment (60 °C) versus angle of inclination.

At 40° angle of inclination wear showed negative value which confirmed that the embedment of sand particles was higher than the material removed from the coating. In the other hand, the embedded sand particles in the coating surfaces formed a relatively hard layer which could resist the abrasive action of sand particles. Increasing the temperature of the heat treatment up to 60 °C caused further enhancement in wear resistance, Fig. 4, where the coating of 0.11 mm thickness displayed minimum wear at 40° and 60° angle of inclination. The degree of embedment increased at that temperature.

Coating of the test specimens by coating (B) showed significant wear increase, Fig. 5. The thicknesses were 0.05, 0.16 and 0.25 mm. The lowest thickness showed lowest wear. Heat treatment of the coating showed no change in wear, Fig. 6, where the lowest thickness displayed the lowest wear and as the thickness increased wear increased. Maximum wear values were displayed at 60° angle of inclination. Increasing the temperature of heat treatment up to 60 °C caused significant wear decrease, Fig. 7. The smallest coating showed the lowest wear.

Wear of coating (C) is shown in Fig. 8. At low angle of inclination the coating showed relatively high wear resistance. This means that the shear strength of the coating is relatively high. As the angle of inclination increased wear increased. Heat treatment of the coating (C), Fig. 9, slightly decreased wear, where minimum values were observed at 60° angle of inclination. The lowest wear was observed for the thicker coating. As the coating thickness decreased wear increased. Increasing the temperature of heat

treatment disturbed the wear of the coating (C), Fig. 10. As the angle of inclination increased wear showed an increasing trend. Generally, the values of wear were relatively lower than the other tested coatings.

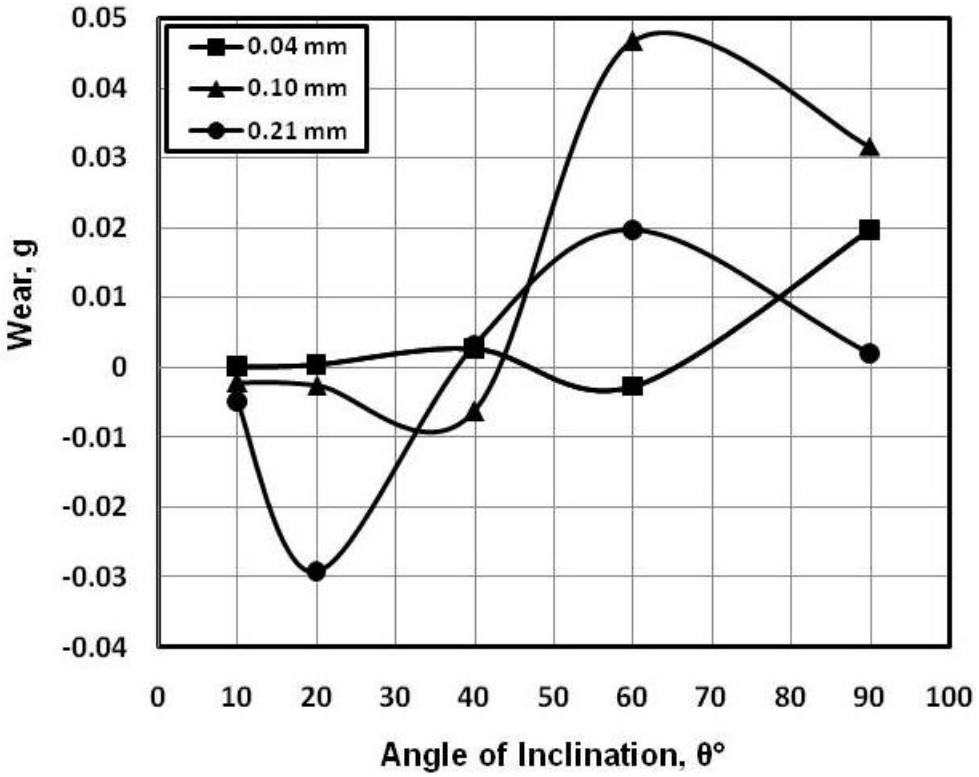

Fig. 8 Wear of coating (C) versus angle of inclination.

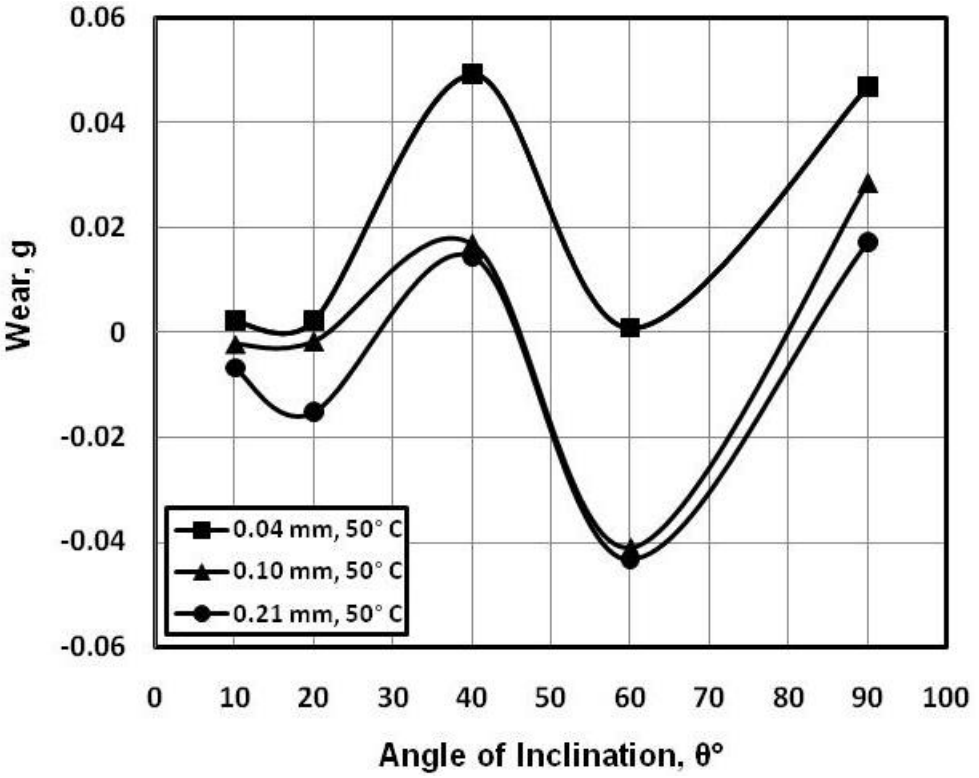

Fig. 9 Wear of coating (C) after heat treatment (50 °C) versus angle of inclination.

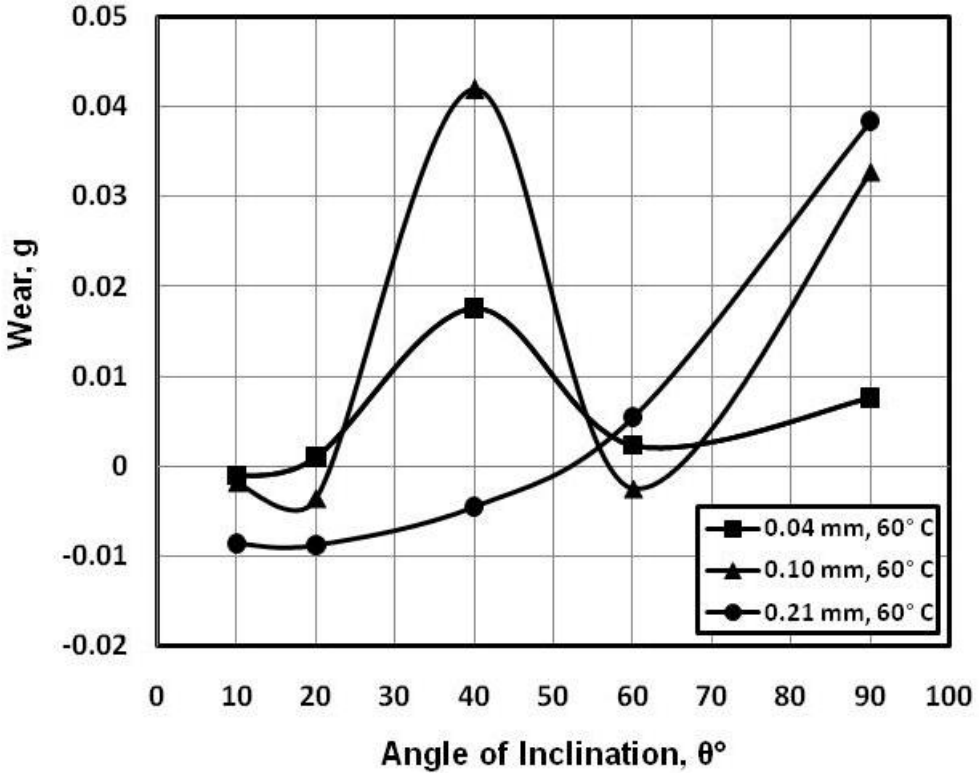

Fig. 10 Wear of coating (C) after heat treatment (60 °C) versus angle of inclination.

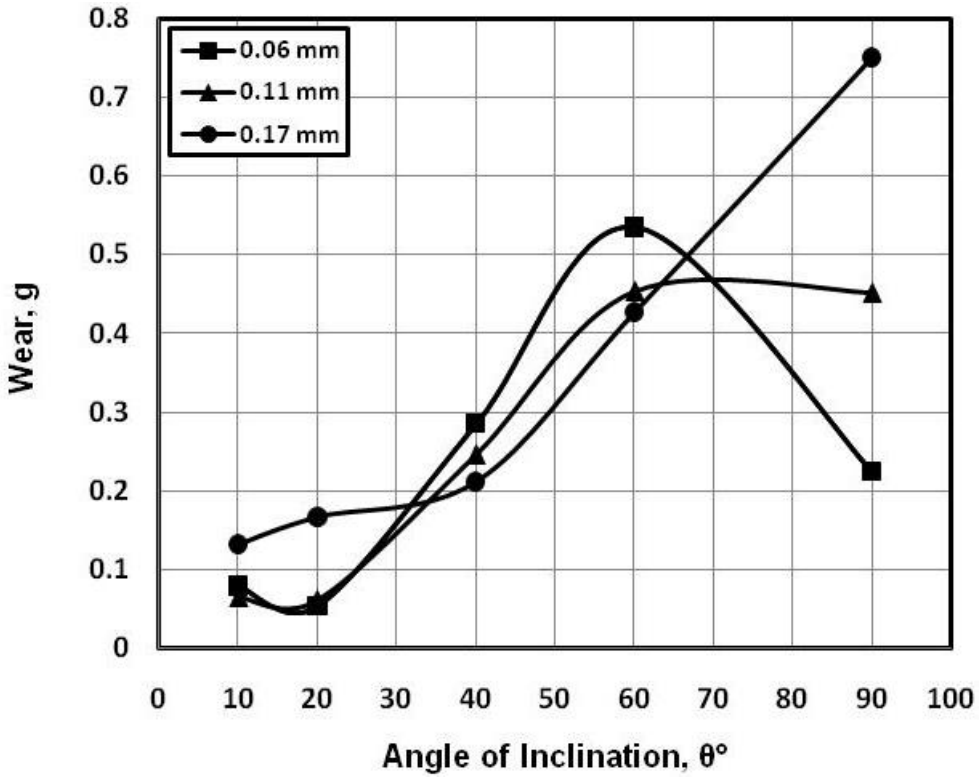

Fig. 11 Wear of coating (D) versus angle of inclination.

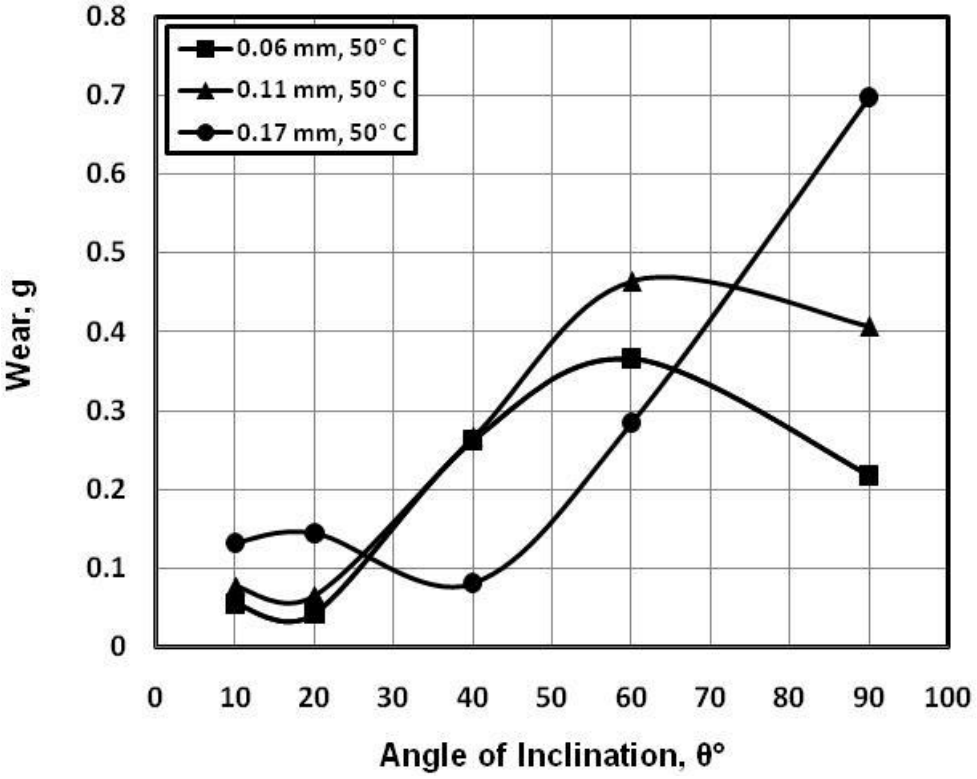

Fig. 12 Wear of coating (D) after heat treatment (50 °C) versus angle of inclination.

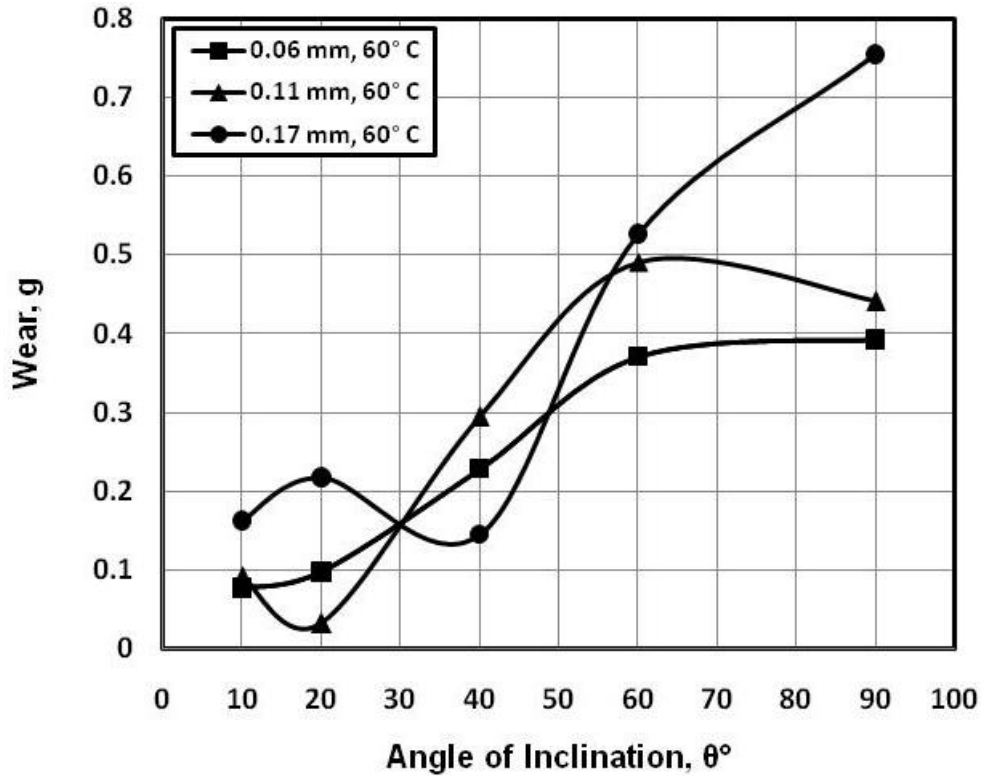

Fig. 13 Wear of coating (D) after heat treatment (60 °C) versus angle of inclination.

Coating (D) displayed remarkable wear increase, Fig. 11. Wear increased as the angle of inclination increased. It seems that the adherence of that coating into the substrate was not enough strong to resist the shear stress caused by erosive sand particles. Heat treatment of the coating (D) up to 50 ° displayed no change in wear, Fig. 12. The thicknesses of the tested coating were 0.06, 0.11 and 0.17 mm. The coatings of thicknesses 0.06 and 0.11 mm showed maximum wear at 60°, while the thicker coating displayed the proportional wear increase with increasing angle of inclination. The same trend of heat treated coatings at 50 °C was observed at 60 °C, Fig. 13. This behavior indicated that the coating did not affected by the heat treatment. Wear of the coating depended on its thickness, where wear increased with increasing coating thickness.

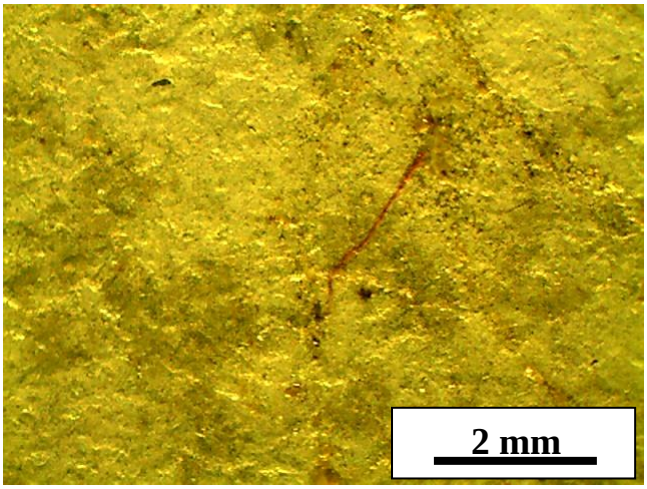

Fig. 14 Coating (B), 60°C, 90° angle of inclination, 0.12 mm coating thickness.

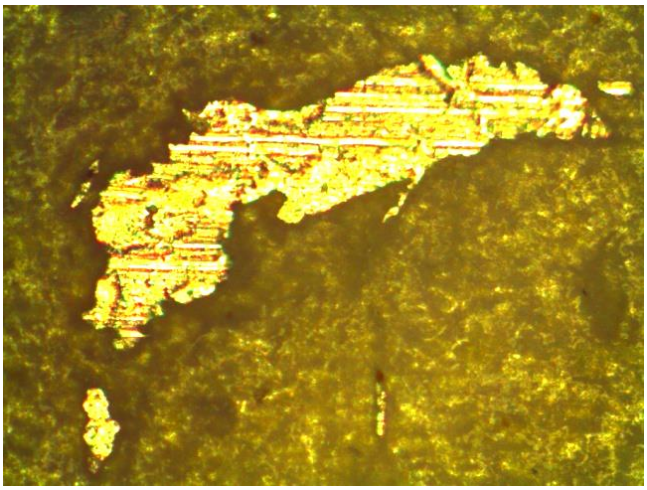

Fig. 15 Coating (B), no heat treatment, 60° angle of inclination, 0.12 mm coating thickness.

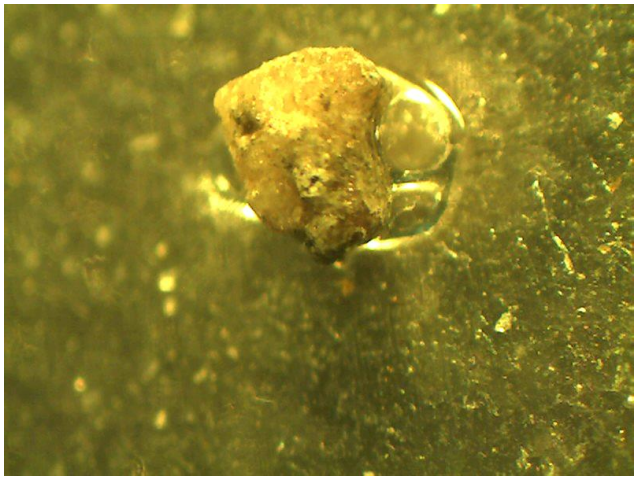

Fig. 16 Coating (C), no heat treatment, 40° angle of inclination, 0.04 mm coating thickness.

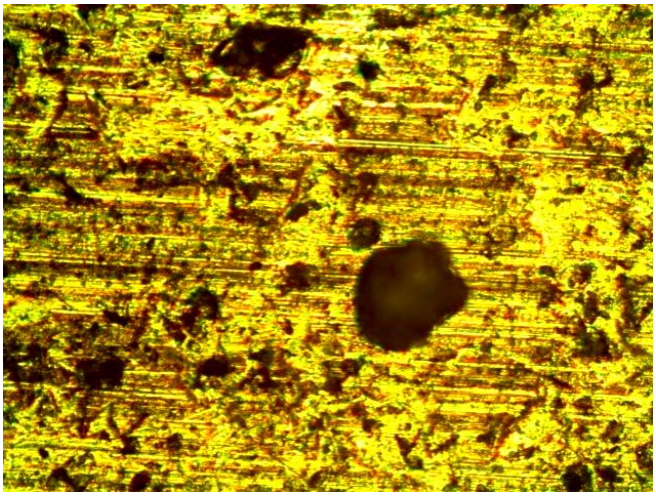

Fig. 17 Coating (C), no heat treatment, 40° angle of inclination, 0.1 mm coating thickness.

The photomicrographs of the surfaces of the tested coatings after tests are shown in Figs. 14 – 17. The photomicrograph of coating (B), after heat treatment at 60°C, 90° angle of inclination, coating thickness = 0.12 mm is shown in Fig. 14. The damage caused by sand particles was insignificant. Complete coating removal followed by severe abrasive wear of steel substrate is shown for coating (B), Fig. 15. Embedment of relatively big sand particles in coating (C) is illustrated in Figs. 16 and 17. The surface damage caused by the sand particles is depending on the degree of embedment of sand particles into the coating surfaces, the coating type, coating thickness, angle of inclination of the tested specimens and heat treatment of the tested coatings.

CONCLUSIONS

1. The highest thickness of coating (A) displayed the minimum wear at 60° angle of inclination. This behavior might be attributed to the increase of embedment of sand in the coating surface with increasing its thickness. Heat treatment of coating (C) up to 50 °C enhanced the wear resistance of the coating. Increasing the temperature of the heat treatment up to 60 °C caused further enhancement in wear resistance.

2. Coating (B) showed significant wear decrease. The lowest wear values were observed for coating thickness of 0.08 mm. At 90° angle of inclination embedment of sand particle was indicated by the weight increase after test. Heat treatment of the coating caused significant wear decrease. Wear decreased down to minimum then remarkably increased with increasing angle of inclination.

3. Coating (C) at low angle of inclination the coating showed relatively high wear resistance. This means that the shear strength of the coating is relatively high. As the angle of inclination increased wear increased. Heat treatment of coating (C) slightly reduced wear, where minimum values were observed at 60° angle of inclination.

REFERENCES

1. Feuerstein A., Kleyman A., "Ti–N multilayer systems for compressor airfoil sand erosion protection ", Surface & Coatings Technology 204 , pp. 1092 – 1096, (2009) .

2. Kleis I., Kulu P., "Solid particle erosion", Springer-Verlag London Limited, (2008).

3. Brendel T., Heutling F., Eichmann W., Uecker M., Uehlein T., "The Engine Yearbook", Aviation Industry Press, London, (2008).

4. Celotta D. W., Qureshi U. A., Stepanov E. V., Goulet D. P., Hunter J., Buckberry C. H., Hill R., Sherikar S.V., Moshrefi-Torbati M., Wood R. J. K., "Sand erosion testing of novel compositions of hard ceramics" , Wear 263 , pp. 278 – 283 , (2007) .

5. Wheeler D. W., Wood R. J. K., "Erosion of hard surface coatings for use in offshore gate valves", Wear 258, pp. 526 – 536, (2005).

6. Wheeler D. W., Wood R. J. K., "Solid particle erosion of diamond coatings under non-normal impact angles", Wear 250, pp. 795 – 801, (2001).

7. Allen C., Sheen M., Williams J., Pugsley V.A., "The wear of ultrafineWC-Co hard metals", Wear 250, pp. 604 – 610, (2001).

8. Sapate S. G., Rama Rao A. V., "Effect of erodent particle hardness on velocity exponent in erosion of steels and cast irons", Mater. Manuf. Processes 18, pp. 783 – 802, (2003).

9. Bose K., Wood R. J. K., "High velocity solid particle erosion behaviour of CVD boron carbide on tungsten carbide", Wear 258, pp. 366 – 376, (2005).

10. Jana B. D., Stack M. M., "Modelling impact angle effects on erosion–corrosion of pure metals: construction of materials performance maps", Wear 259, pp. 243 - 255, (2005).

11. Barik R. C., Wharton J. A., Wood R. J. K., Stokes K. R., "Electro-mechanical interactions during erosion–corrosion", Wear 267, pp. 1900 - 1908, (2009).

12. Wong Ch. Y. , Solnordal C., Swallow A., Wang S., Graham L., Wu J., "Predicting the material loss around a hole due to sand erosion " , Wear 276–277 , pp. 1–15 , (2012) .

13. Wu J., Graham L. J. W., Lester D., Wong C. Y., Kilpatrick T., Smith S., Nguyen B., "An effective modeling tool for studying erosion", Wear 270, pp. 598 - 605, (2011).

14. Gnanavelu A., Kapur N., Neville A., Flores J. F., "An integrated methodology for predicting material wear rates due to erosion", Wear 267, pp. 1935 – 1944, (2009).

15. Neaman, R. and Anderson, A., "Development and Operating Experience of Automatic Pulse-Jet Self-Cleaning Air Filters For Combustion Gas Turbines", ASME paper 80, GT, (1980).